



Defining total-body AIDS-virus burden with implications for curative strategies

Jacob D Estes¹, Cissy Kityo², Francis Ssali², Louise Swainson³, Krystelle Nganou Makamdop⁴, Gregory Q Del Prete¹, Steven G Deeks⁵, Paul A Luciw⁶, Jeffrey G Chipman⁷, Gregory J Beilman⁷ , Torfi Hoskuldsson⁷, Alexander Khoruts⁸, Jodi Anderson⁸, Claire Deleage¹, Jacob Jasurda⁸, Thomas E Schmidt⁸, Michael Hafertepe⁸, Samuel P Callisto⁸ , Hope Pearson⁸, Thomas Reimann⁸, Jared Schuster⁸, Jordan Schoepfoerster⁸, Peter Southern⁹, Katherine Perkey⁹, Liang Shang⁹, Stephen W Wietgreffe⁹, Courtney V Fletcher¹⁰, Jeffrey D Lifson¹, Daniel C Douek⁴, Joseph M McCune³, Ashley T Haase⁹ & Timothy W Schacker⁸

In the quest for a functional cure or the eradication of HIV infection, it is necessary to know the sizes of the reservoirs from which infection rebounds after treatment interruption. Thus, we quantified SIV and HIV tissue burdens in tissues of infected nonhuman primates and lymphoid tissue (LT) biopsies from infected humans. Before antiretroviral therapy (ART), LTs contained >98% of the SIV RNA⁺ and DNA⁺ cells. With ART, the numbers of virus (v) RNA⁺ cells substantially decreased but remained detectable, and their persistence was associated with relatively lower drug concentrations in LT than in peripheral blood. Prolonged ART also decreased the levels of SIV- and HIV-DNA⁺ cells, but the estimated size of the residual tissue burden of 10⁸ vDNA⁺ cells potentially containing replication-competent proviruses, along with evidence of continuing virus production in LT despite ART, indicated two important sources for rebound following treatment interruption. The large sizes of these tissue reservoirs underscore challenges in developing ‘HIV cure’ strategies targeting multiple sources of virus production.

The quest for a cure for HIV infection was inspired by Timothy Ray Brown, an HIV-infected individual who, in the course of treatment for refractory leukemia with total-body irradiation and chemotherapy, also received two bone marrow transplants with CCR5-delta 32-mutated HIV-resistant cells. The combination of decreased HIV reservoirs and introduced resistant cells is thought to have cured not only his leukemia but also his HIV infection¹. The success in Brown's case, despite being achieved with a highly toxic treatment, has galvanized the field to seek a functional cure (i.e., a prolonged period off ART without detectable plasma viremia) or HIV eradication through safer and more scalable approaches.

What are the cellular and anatomic compartments from which infection might rebound after ART and achieve a functional cure or eradication? To answer that question, we performed an extensive analysis of potential sources of viral rebound, using both established and next-generation *in situ* hybridization (ISH) technologies and quantitative image analysis. We paid particular attention to LTs in HIV and simian immunodeficiency virus (SIV) infections, in which CD4⁺ T cells in the gut and secondary LT have previously been shown to be the principal sites where most of the cells producing viral (v) RNA (vRNA⁺ cells) are found in HIV-infected humans and SIV-infected

macaques^{2–18}, and where there is a very large pool (more than 10¹⁰ cells) of transcriptionally silent vDNA⁺ cells in LTs³, some of which contain replication-competent proviruses.

Although previous characterizations of HIV- and SIV-infected tissues have clearly identified LT and the vDNA⁺ and vRNA⁺ cells therein as important anatomic sites and cellular sources of virus potentially capable of reigniting infection after treatment interruption^{2–4,7,14,16,18,19}, much of this work was done during the 1990s, before modern ART. Understanding of the extent to which current ART regimens affect virus burden in LT and other tissues is therefore incomplete. Moreover, recent evidence has indicated that even contemporary ART regimens that suppress viral replication and decrease plasma viremia to levels below the sensitivity of clinical laboratory assays achieve lower drug levels in LT than the fully suppressive drug levels in peripheral blood (PB)⁵. These lower tissue drug levels are correlated with incomplete suppression of viral replication in LT in some patients^{19,20}. There is also growing appreciation that the size of the pool of latently infected cells that may contribute to viral rebound after treatment interruption has been underestimated by as much as 70-fold (ref. 21). There are thus three good reasons to reexamine potential sources of rebound when ART is interrupted.

¹AIDS and Cancer Virus Program, Frederick National Laboratory for Cancer Research, Leidos Biomedical Research, Inc., Frederick, Maryland, USA. ²Joint Clinical Research Center, Kampala, Uganda. ³Division of Experimental Medicine, University of California, San Francisco, San Francisco, California, USA. ⁴Vaccine Research Center, National Institutes of Health, Bethesda, Maryland, USA. ⁵Department of Medicine, University of California, San Francisco, San Francisco, California, USA. ⁶Department of Pathology and Laboratory Medicine, University of California, Sacramento, Sacramento, California, USA. ⁷Department of Surgery, University of Minnesota, Minneapolis, Minnesota, USA. ⁸Department of Medicine, University of Minnesota, Minneapolis, Minnesota, USA. ⁹Department of Microbiology and Immunology, University of Minnesota, Minneapolis, Minnesota, USA. ¹⁰College of Pharmacy, University of Nebraska Medical Center, Omaha, Nebraska, USA. Correspondence should be addressed to T.W.S. (schacker@umn.edu).

Received 22 December 2016; accepted 25 August 2017; published online 2 October 2017 ; doi:10.1038/nm.4411

To identify the sources of potential viral rebound, we conducted extensive analysis of necropsy tissues from rhesus macaques (RMs) infected with SIVmac251, SIVmac239, or RT-SHIV, by using the new easily performed techniques of DNAscope and RNAscope ISH to quantify vDNA⁺ and vRNA⁺ cells²²; a previously described ISH method using tyramide signal amplification (TSA) to score for virus-producing cells²³; and measurement of the intracellular concentrations of ART drugs and/or active metabolites to assess associations between suboptimal tissue drug concentrations and ongoing replication during ART. In HIV infection, we examined LT reservoirs in serial lymph node (LN) and gut biopsies obtained before and after at least 2 years of ART in HIV-infected people. We found that, in a nonhuman primate (NHP) model, in the absence of ART, >98% of detectable vRNA⁺ and vDNA⁺ cells were in LT. ART decreased the frequency of vRNA⁺ cells, but, despite apparently clinically effective ART (plasma vRNA <50 copies/mL), vRNA⁺ cells were detected in every organ system examined. In LN, in which tissue levels of ART drugs are substantially lower than those in PB, we found that virus-producing cells remained detectable, and we provide new estimates of the potential size of the pool of vDNA⁺ cells in LTs with replication-competent proviruses. The persistence of virus-producing cells after ART and a large pool of vDNA⁺ cells with the potential to become reactivated underscores the challenges of HIV eradication.

RESULTS

NHP studies

We analyzed brain, gut, heart, kidney, liver, lung, LN, and spleen tissues collected in necropsies of eight RMs infected with SIVmac251 (three untreated and five subjected to ART) and housed at Advanced Bioscience Laboratories. The three untreated SIVmac251-infected animals were euthanized and necropsied at 14, 43, or 90 d postinfection (dpi). The remaining five SIVmac251-infected animals were euthanized and necropsied after 20–22 weeks of treatment with raltegravir, darunavir (DRV), ritonavir (RTV), emtricitabine (FTC), and tenofovir (TFV) starting at 56 dpi (**Supplementary Fig. 1a**). We also analyzed LN from 11 SIVmac239-infected RMs housed at the US National Institutes of Health (NIH) on suppressive ART regimens (described in the methods section and previous publications^{22,24,25}; **Supplementary Fig. 1b,c**); tissues from four untreated juvenile RMs infected with reverse transcriptase–SIV expressing HIV-1 envelope (RT-SHIV) and housed at the California National Primate Research Center (CNPRC), euthanized and necropsied at 19, 24, 41, or 69 weeks after infection; and tissues from four RT-SHIV-infected juvenile RMs housed at the CNPRC, after a minimum of 26 weeks of ART with a combination of efavirenz, FTC, and TFV²⁶ (**Supplementary Fig. 1d**). We assessed the tissue virus burden in a total of 27 RMs infected with three distinct simian AIDS viruses.

Reservoir measurements by ISH

We used ISH technologies and quantitative image analysis to define tissue reservoirs in SIV/SHIV and HIV infections on the basis of numbers of vDNA⁺, vRNA⁺, and virus-producing cells. These cellular measurements thus defined reservoirs in a different way from PCR and RT-PCR analysis of nucleic acids extracted from homogenized whole tissues, in which there is ambiguity in attributing the number of copies of vDNA or vRNA to either a large number of cells with a few viral copies or to a small number of cells with a large number of viral copies. We used four methods of ISH: (i) ³⁵S-radiolabeled riboprobes that hybridize to regions spanning the genome of SIV/SHIV (*gag*, *pol*, *vif*, *vpr*, *env*, and *nef*), to detect transcriptionally active vRNA⁺

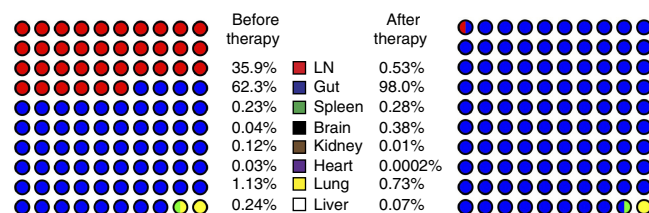


Figure 1 Graphical representation of the proportion of vRNA⁺ cells in each organ system before and during suppressive ART.

cells that we have previously shown to contain both unspliced and spliced vRNAs⁸; (ii) digoxigenin-labeled riboprobes combined with TSA amplification, to reveal virus-producing cells under light microscopy²³; (iii) RNAscope ISH, an ISH technique more rapid than the ³⁵S technique but with comparable sensitivity and specificity²², to determine the frequency of vRNA⁺ cells/g tissue; and (iv) DNAscope ISH²², to measure the frequency and location of vDNA⁺ cells. DNAscope enables sensitive detection and quantification of vDNA⁺ cells, yielding results comparable to those of *in situ* PCR^{2,3} but with greater speed, convenience and higher spatial resolution of the vDNA signal within infected cells. We compared the frequency of vRNA⁺ and vDNA⁺ cell/g LT to measurements of vRNA and vDNA by qRT-PCR and qPCR, and found excellent agreement ($R^2 = 0.89$ and $P < 0.0001$ for RNA and $R^2 = 0.73$ and $P < 0.0001$ for DNA; **Supplementary Fig. 2**). The agreement with similar recently published results²² provided further justification for this approach to quantifying viral reservoirs on a cellular basis *in situ*.

SIV RNA⁺ cells are mainly in lymphoid tissues

We quantitatively characterized cellular tissue reservoirs in untreated SIV infection in the brain, heart, kidney, liver, lung, spleen, LNs (axillary, colonic, inguinal, and mesenteric), and multiple sites in the gut (duodenum, jejunum, ileum, ascending and transverse colon, and rectum) (representative images of SIV *in situ* hybridization from multiple tissues through two complementary approaches in **Supplementary Fig. 3**). We analyzed serial 4- μ m sections of formalin-fixed, paraffin-embedded tissues, evaluating every fifth section in a total of at least five sections to provide analysis through $\geq 80 \mu$ m of each tissue. The frequency of SIV RNA⁺ cells was determined in each section and converted to the frequency per g on the basis of the measured area of the section, nominal thickness, and previously determined density of fixed tissue of ~ 1 g/cm (refs. 3,16). For example, the frequency of vRNA⁺ cells/ μ m² area $\times 4 \mu$ m thick = vRNA⁺ cells/ μ m³ $\times 10^{12} \mu$ m³/cm³ $\times 1$ g/cm³ = vRNA⁺ cells per g tissue.

The density of vRNA⁺ cells was highest in LT, but vRNA⁺ cells were detected in every organ, including the heart, liver, and kidney, and the central nervous system. To estimate the total virus burden for different tissues, we assumed that each organ contributes vRNA⁺ cells to the total population of vRNA⁺ cells in an amount proportional to the frequency of vRNA⁺ cells measured by ISH and the total mass of these organs. In the RMs studied at peak viremia, for example, the mass of the heart was approximately 38.3 g, and the frequency of vRNA⁺ cells was 7.54×10^3 cells/g; thus, the total number of infected cells in this organ was accordingly estimated at $\sim 2.89 \times 10^5$ cells (**Supplementary Table 1**). The combined mass of lymph nodes for this animal was estimated to be 78 g ($\sim 1\%$ of total body mass). With a mean frequency of $\sim 8.73 \times 10^5$ vRNA⁺ cells/g, the total population of vRNA⁺ cells in LNs was estimated at 7.68×10^7 cells, approximately 2 log₁₀ higher than that found in the heart. In the gut, we measured $\sim 5.57 \times 10^5$

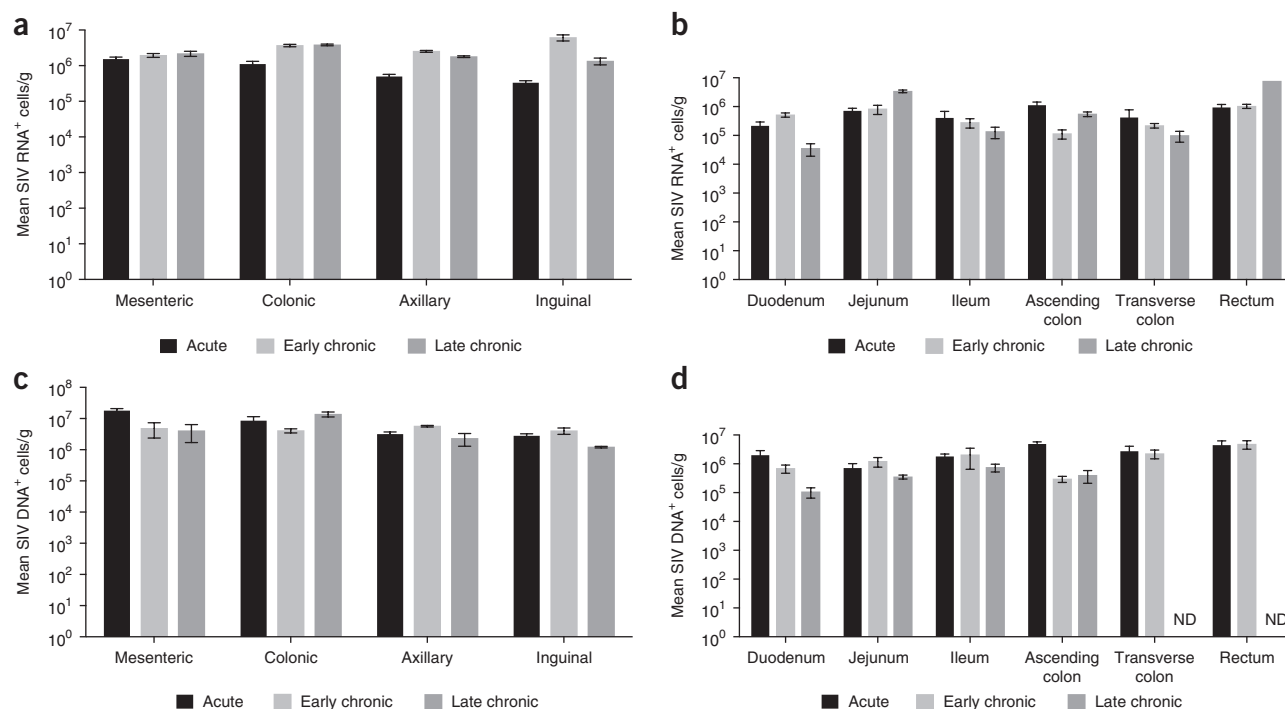


Figure 2 Quantitative image analysis of SIV vRNA⁺ cells in untreated SIV infection. **(a,b)** Estimated frequency of vRNA⁺ cells/g tissue in LN-associated **(a)** and gut-associated **(b)** LT in an animal sampled during acute, early-chronic and late-chronic stages of infection. **(c,d)** Estimated frequency of SIV DNA⁺ cells in four different LNs **(c)** and seven sites in GALT **(d)** at each stage of SIV infection from the same animals. Each value is from a single LN from a single animal, with an average of five sections made. Error bars, s.e.m. of the five measurements. ND, none detected.

vRNA⁺ cells/g; thus, on the basis of the total organ weight of 315 g in this animal, $\sim 1.68 \times 10^8$ vRNA⁺ cells, or more than two-thirds of the total number of vRNA⁺ cells in all of the organs examined, were in the gut. The contribution of each organ to the estimated total population of infected cells (as a percentage of the total) before and during ART (graphically shown in **Fig. 1**) illustrated that the primary reservoir sites of infection were LTs, in which $\sim 98.4\%$ of the vRNA⁺ cells resided (gut, LNs, and spleen). The addition of the lung, a tissue with abundant mucosal-associated LT, increased our estimate of the frequency of vRNA⁺ cells residing in LTs to $\sim 99.6\%$.

vRNA⁺ and vDNA⁺ cell populations are established in LT reservoirs in early infection

We investigated differences in the frequency of viral nucleic acid-positive cells on the basis of anatomic site and duration of untreated SIVmac251 infection in four LNs (axillary, colonic, inguinal, and mesenteric) and from multiple sites in the gut (duodenum, jejunum, ileum, ascending colon, transverse colon, and rectum) in the acute (14 dpi), early (43 dpi), and later chronic stages (90 dpi) of infection. In the LN and gut, vRNA⁺ cells were detected in early infection and varied by only approximately 0.5 log (**Fig. 2a,b**), and we found remarkable consistency among LNs located in different anatomic locations. The estimated frequency of vDNA⁺ cells in LT in the SIVmac251-infected animals, assessed with SIV DNAscope (**Fig. 2c,d** and **Supplementary Fig. 4**), also showed that substantial pools of vDNA⁺ cells were established early and maintained at high levels in the chronic stages of infection in RMs.

Effects of ART on vRNA⁺ and vDNA⁺ cell populations in tissues

In SIVmac251-infected RMs that received 20–22 weeks of ART beginning at 56 dpi, as compared with those with untreated infections, the

frequency of vRNA⁺ cells decreased by approximately 2 log₁₀ in LNs (**Fig. 3a** and **Supplementary Table 2a–d**) but by only approximately twofold or less in the gut and spleen. The frequency of vRNA⁺ cells was actually higher in the brains of animals receiving ART compared with untreated animals, a result presumably reflecting interanimal variability (**Supplementary Table 2a**) and poor penetration of drugs into the brain. In the RT-SHIV-infected animals, 26 weeks of ART decreased the number of vRNA⁺ cells by ~ 3 to 4 log₁₀ in all LT, but by only approximately twofold in the brain (**Fig. 3b**). The greater decreases seen in the RT-SHIV-infected animals compared with SIV-infected animals may reflect the relative effectiveness of the different ART regimens against the respective target viruses, distinct differences in viral replication capacity in RMs, differences in tissue concentrations of ART, or Env-specific immune responses.

We have previously shown in HIV-infected humans that the intracellular concentrations of antiretroviral drugs (ARVs) in LT can be significantly less than the concentrations in peripheral blood mononuclear cells (PBMCs) and well below the optimal concentration for viral suppression⁵. We measured intracellular concentrations of ARVs in PBMCs and cells of the LN, ileum (gut-associated lymphoid tissue (GALT)) and rectal-associated mucosal tissue (RALT) from six of the animals described above and similarly found lower ART concentrations in LT than in blood (**Fig. 4**). The median ratios for TFV-diphosphate (TFV-DP, an active phosphorylated form of the drug) were 0.84 for LN/PBMCs, 0.41 for GALT/PBMCs, and 0.84 for RALT/PBMCs. The median ratios for FTC-triphosphate (FTC-TP) were 0.26 for LN/PBMCs, 0.32 for GALT/PBMCs, and 0.32 for RALT/PBMs. The median RALT/PBMC ratio for DRV was 15; however, DRV was not quantifiable in LN or GALT samples. Thus, the concentrations of the ARVs were not equivalent to those in peripheral blood in any of the studied compartments, with the exception of DRV

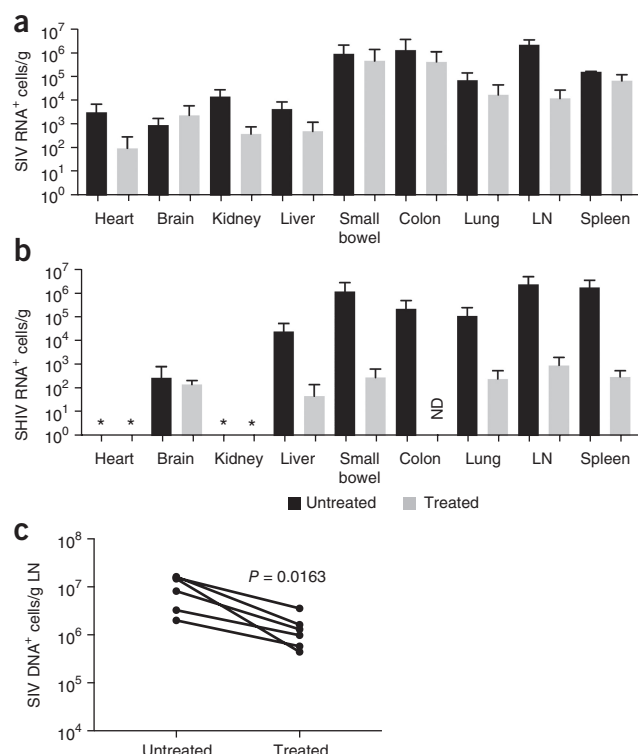


Figure 3 Quantitative image analysis of vRNA⁺ and vDNA⁺ cells in groups with untreated and treated SIV and SHIV infections. (a) Frequency (mean frequency and s.d.) of SIVmac251 RNA⁺ cells in 3 untreated RMs (euthanized at 14, 43, and 90 dpi) and 5 RMs after 20–22 weeks of ART starting at 56 dpi. (b) Frequency of vRNA⁺ cells in 4 RT-SHIV-infected animals before ART and in 4 RT-SHIV-infected animals after 26 weeks of ART. (c) Frequency of SIV DNA⁺ cells in paired lymph nodes of five SIVmac239-infected RMs before and after 26 weeks of ART (comparison by two-tailed paired *t* test). Asterisks, tissue not available; ND, none detected.

in RALT (summary of intracellular concentration of ARVs for all drugs studied in **Supplementary Table 3**). These results support the hypothesis that comparatively lower ARV concentrations in different tissues may contribute to incomplete suppression of viral replication in those tissues.

With the exception of the heart tissues, vRNA⁺ cells were detectable in every animal on ART, even though all had plasma viral loads <50 copies/mL (the limit of detection of the assay used). The highest numbers of vRNA⁺ cells during ART were mainly in LTs (LN, spleen, and GALT) and the lung. Because detection of vRNA⁺ cells signifies transcription and not necessarily virus production, we used ISH/TSA amplification with an enzyme-linked immunofluorescence technique (ELF97) to detect virus-producing cells through light microscopy²³, to show that vRNA⁺ cells also produced virus during ART. We measured the frequency of vRNA⁺ cells with RNAscope and the frequency of cells producing virions with TSA/ELF97 in 20 sub-adjacent sections from two of the SIVmac251-infected animals on suppressive ART for >6 months (**Fig. 5**). There was good agreement between the two measurements (**Supplementary Table 4**), a result consistent with the conclusion that most vRNA⁺ cells detected in LN were producing virions.

We used DNAscope to assess the effects of ART on the frequency of vDNA⁺ cells in 11 SIVmac239-infected animals that had been treated for a mean of 30 weeks (range 25–35 weeks) beginning at 4 weeks postinfection (wpi) (**Fig. 3c** and **Supplementary Fig. 4**).

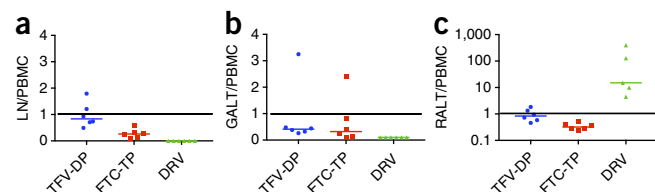


Figure 4 Intracellular concentrations of TFV-DP, FTC-TP, and DRV in LNs, gut, and rectum, as compared with simultaneous measurements in PBMCs in six RMs. (a) LN/PBMCs. (b) Gut/PBMCs. (c) Rectum/PBMCs. Median concentrations are indicated by horizontal lines.

Before ART, the mean frequency of vDNA⁺ cells was $\sim 1 \times 10^7$ cells/g LT. ART decreased the mean frequency of vDNA⁺ cells/g by $\sim 1.7 \log_{10}$ to $\sim 3.5 \times 10^5$ cells/g LT. Thus, there was a very large residual reservoir of vDNA⁺ cells during ART, the implications of which are discussed below.

HIV RNA⁺ and DNA⁺ cells in LT

To compare residual virus levels in LT in SIV infection with those in HIV infection of humans, we analyzed LN and rectal samples collected before ART and after at least 2 years of ART from a cohort of 20 people in Kampala, Uganda. These individuals had advanced infection when ART was begun, in accordance with treatment guidelines in Uganda at the time when tissues were obtained. The average age of this cohort at entry was 32 years, and 50% were women. The mean CD4⁺ T cell count at the beginning of the study was 174 cells/mm³ (range 30–309 cells/mm³), and the mean plasma HIV viral load was 8.1×10^4 copies/mL (range 7.4×10^2 to 9.1×10^5 copies/mL) (individual changes in CD4 and plasma viral loads over time for a subset of 14 individuals followed longitudinally in **Supplementary Figs. 5** and **6**, respectively).

On the basis of preliminary analyses in which we found that clade B riboprobes detected fewer vRNA⁺ cells than did riboprobes for the prevalent clades A and D in Uganda (data not shown), we designed RNAscope and DNAscope probes specific to clades A and D for this study. With these probes, we determined an average frequency of vRNA⁺ cells in the LN and rectum before ART of $\sim 9.4 \times 10^4$ cells/g (6.3×10^3 to 3.5×10^5 cells/g) and $\sim 2.5 \times 10^5$ cells/g (2.3×10^4 to 9.6×10^5 cells/g), respectively (**Fig. 6a**), a result in reasonable agreement with previous estimates of $\sim 5 \times 10^4$ /g in LNs of HIV-infected patients in the United States, with a mean CD4⁺ T cell count of 400 cells/ μ L (ref. 16). However, this value was more than tenfold lower than that observed in the SIVmac251-infected RMs necropsied at 90 dpi.

To determine the size of the vDNA⁺ cell population before ART in relation to vRNA⁺ cells (as an estimate of cells with transcriptionally competent proviruses in these snapshots), we performed DNAscope and RNAscope in LN and rectum specimens. Before ART, the mean frequency of vDNA⁺ cells in LN was $\sim 6.2 \times 10^7$ vDNA⁺ cells/g LT (range 8.3×10^6 to 1.3×10^8) (**Fig. 6b**), and thus the ratio of vRNA⁺ cells to vDNA⁺ cells was ~ 0.002 , in good agreement with the ratios of 1:100 to 1:400 determined in previous studies using *in situ* PCR and ISH².

ART had a significant effect on the LT reservoir in individuals who had been treated for >2 years (range 2–6 years) and had undetectable plasma viral loads (<40 copies/mL in the first 12 months of the study and then <20 copies/mL). The mean frequency of vDNA⁺ cells declined by $\sim 3 \log$, to $\sim 2.7 \times 10^5$ cells/g (range 1.2×10^5 to 4.5×10^5 cells/g; $P = 0.0237$, analysis of variance (ANOVA)). In gut tissues, however, we did not observe a significant decrease in the size of the vDNA⁺-cell reservoir (**Fig. 6c**): before ART, the frequency of vDNA⁺ cells was

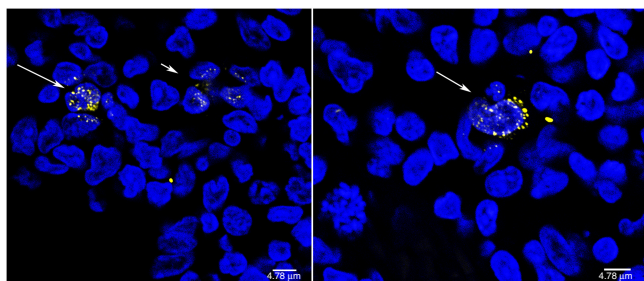


Figure 5 Virus-producing cells in two SIV-infected RMs during ART, detected by ISH/TSA. At left, the long arrow points to two virus-producing cells; the short arrow points to a cluster of four productively infected cells. At right, the arrow points to two productively infected cells. Yellow, virus particles; blue, cell nuclei. Multiphoton images were obtained at z steps of 0.1 μm and subsequently filtered to decrease the intracellular viral RNA staining and make virus particles visible. The sizes of virions depend on the plane of focus; larger virions are in focus.

$\sim 3.2 \times 10^5$ cells/g LT (range 2.8×10^5 to 3.4×10^5) compared with a mean of $\sim 2.7 \times 10^5$ cells/g (range 1.5×10^5 to 4.3×10^5 cells/g) after >62 months of ART (range 2–6 years; $P > 0.05$).

DISCUSSION

Using contemporary ISH methodologies to analyze tissue virus burdens as populations of infected cells, we confirmed the paramount importance of the LT reservoir before and during ART. These technologies also notably revealed that, during ART, vRNA⁺ and virus-producing cells persist in tissues with plasma viremia of fewer than 50 copies/mL. Thus, our findings suggest that tissue assessments will be needed to fully determine the effectiveness of interventions designed to cure HIV infection.

In the NHP models in which we were able to comprehensively analyze key organ systems in a way that would not be possible in HIV-infected humans, $\sim 99.6\%$ of the SIV RNA⁺ cells were found in LTs (LNs, gut, spleen, and lung). Thus, there is now compelling additional evidence supporting the conclusion that lymphoid organs are the principal tissue sites of virus production⁷. In the heart, liver, and kidney, the frequencies of vRNA⁺ cells were very low, but we did find vRNA⁺ cells in the brain (cortex) at a frequency of $\sim 2.3 \times 10^4$ cells/g, and the frequency was comparable or higher in animals on ART, in agreement with a potentially important role of the brain as a site of viral persistence that may not be as amenable as peripheral tissues to viral suppression by ART, at least with the ARVs used in the present study^{27,28}.

In both SIV-infected RMs and HIV-infected people, ART suppressed viral replication, as evidenced by plasma vRNA measurements, but we

readily detected vRNA⁺ and virus-producing cells in tissues, albeit at lower frequencies than those in untreated animals. This evidence of continued low-level virus production despite ostensibly suppressive ART was correlated, particularly in the gut, with the lower relative concentrations of ARVs in tissues compared with PBMCs documented in these studies. Notably, our results are consistent with the conclusions from studies of HIV infection indicating that suboptimal tissue levels of ARVs in some treated infected individuals may not fully suppress virus production in tissues^{5,20}. In the Ugandan cohort, other factors such as tissue fibrosis, persistent gastrointestinal-tract damage and associated inflammation and greater CD4⁺ T cell depletion in advanced stages of infection at the time at which ART was initiated^{29–33} may also have contributed to ongoing infection by further lowering drug levels and impairing containment of infection by the damaged immune system.

The presence of vRNA⁺ cells in tissues during ART does not distinguish between low levels of ongoing virus production and reactivation of latently infected cells. What we can conclude from the estimated quasi-steady-state whole-body burden of 7 million vRNA⁺ cells in LT snapshots in people on suppressive ART for >2 years is that either or both reservoirs are large immediate sources of virus that can reignite infection after treatment interruption. This conclusion is supported by the rapid multifocal rebound observed in LT with genetically diverse viruses with treatment interruption¹⁹ in HIV-infected people on ART for an average of 14.6 years, and by the estimates determined in this study of the size of the pool of latently infected cells containing replication-competent and inducible proviruses. We found a frequency of vDNA⁺ cells maintained in the LT reservoir at levels of $\sim 10^5$ vDNA⁺ cells/g despite ART in both SIV and HIV infections. If, as recent estimates have suggested²¹, only $\sim 5\%$ of vDNA⁺ cells have replication-competent and inducible proviruses, the total-body burden of latently infected cells with potentially inducible replication-competent proviruses would be $\sim 4 \times 10^8$ cells. This estimate is in excellent agreement with measurements by Bruner *et al.*, whose sequence analysis has suggested that a population of $\sim 1.2 \times 10^7$ resting memory cells in PBMCs contain replication-competent provirus³⁴. Given that fewer than 5% of resting memory cells are in peripheral blood, the frequency of vDNA⁺ cells in LTs with replication-competent provirus would be on the order of $\sim 2.4 \times 10^8$ cells. Thus, two independent methods converge on similar estimates of a very large potentially inducible reservoir in patients on current ART regimens.

Both ongoing low-level virus production due to lower concentrations of ARVs in LTs and reactivation of latently infected cells provide potential sources of virus that may rapidly reignite infection

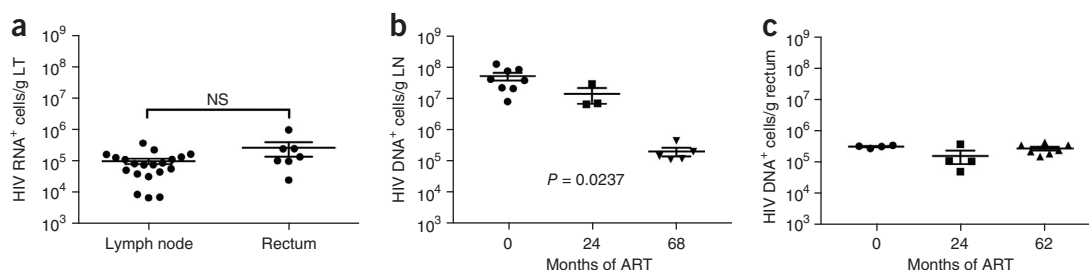


Figure 6 Frequency of vRNA and vDNA⁺ cells/g in LN and rectal biopsies from HIV⁺ Ugandans before and during ART. (a) Frequency of HIV RNA⁺ cells/g in LNs compared with the frequency in the rectum (unpaired *t* test). (b,c) Frequency of DNA⁺ cells in LNs (b) and the rectum (c) after prolonged ART (one-way ANOVA). NS, not significant. Data are shown as mean \pm s.e.m.

after treatment interruption. It will be important in future studies to develop and evaluate cure strategies that effectively target each source. For ongoing virus production, fully suppressive ARTs are needed for LT and other tissue sites. For the latently infected inducible population, strategies with significantly greater efficacy than that afforded by current latency-reversal agents, coupled with effective means to eliminate the reactivated cells, are also needed.

METHODS

Methods, including statements of data availability and any associated accession codes and references, are available in the [online version of the paper](#).

Note: Any Supplementary Information and Source Data files are available in the online version of the paper.

ACKNOWLEDGMENTS

The authors thank S. Povolny and C. Olson for help with manuscript preparation and editing, and the Antiviral Pharmacology Laboratory at the University of Nebraska for quantification of ARV concentrations. This work was supported by grants UL1TR000114 (T.W.S.), AI096109 (J.D.E.), L. Swainson, S.G.D., J.A., J.J., T.E.S., J.M.M., and T.W.S.), OD011107 (P.A.L.), AI124965 (C.V.F.), and AI074340 (J.G.C., G.J.B., T.H., A.K., J.A., J.J., T.E.S., M.H., S.P.C., J.S., C.V.F., A.T.H., and T.W.S.), and in part by federal funds from the National Cancer Institute, National Institutes of Health, under contract no. HHSN261200800001E (J.D.E., C.D., and J.D.L.). The content of this publication does not necessarily reflect the views or policies of the Department of Health and Human Services, nor does mention of trade names, commercial products, or organizations imply endorsement by the US Government.

AUTHOR CONTRIBUTIONS

J.D.E. contributed to study design and oversight, sample analysis, and manuscript preparation. C.K. contributed to study design, oversight of the Uganda cohort, and manuscript preparation. E.S. contributed to management of the Ugandan cohort, including regulatory and sample management. L. Swainson, G.Q.D.P., J.A., C.D., J.J., T.E.S., M.H., S.P.C., H.P., T.R., J. Schuster, J. Schoephoerster, and K.P. contributed to sample analysis. P.S. contributed to sample and data analysis. K.N.M. contributed to sample collection and analysis, and data management. J.G.C., G.J.B., and T.H. performed surgery to collect LN and rectal samples from the Ugandan cohort. A.K. contributed to sample collection and study design. L. Shang performed the TSA/ELF assays and analysis. S.W.W. contributed to data analysis and provided technical support. C.V.F. contributed to drug-level data acquisition, sample analysis, and manuscript preparation. S.G.D., P.A.L., J.D.L., D.C.D., J.M.M., A.T.H., and T.W.S. contributed to study design, data analysis, and manuscript preparation.

COMPETING FINANCIAL INTERESTS

The authors declare no competing financial interests.

Reprints and permissions information is available online at <http://www.nature.com/reprints/index.html>. Publisher's note: Springer Nature remains neutral with regard to jurisdictional claims in published maps and institutional affiliations.

- Yukl, S.A. *et al.* Challenges in detecting HIV persistence during potentially curative interventions: a study of the Berlin patient. *PLoS Pathog.* **9**, e1003347 (2013).
- Embreton, J. *et al.* Analysis of human immunodeficiency virus-infected tissues by amplification and in situ hybridization reveals latent and permissive infections at single-cell resolution. *Proc. Natl. Acad. Sci. USA* **90**, 357–361 (1993).
- Embreton, J. *et al.* Massive covert infection of helper T lymphocytes and macrophages by HIV during the incubation period of AIDS. *Nature* **362**, 359–362 (1993).
- Faust, R.A. *et al.* Outpatient biopsies of the palatine tonsil: access to lymphoid tissue for assessment of human immunodeficiency virus RNA titers. *Otolaryngol. Head Neck Surg.* **114**, 593–598 (1996).
- Fletcher, C.V. *et al.* Persistent HIV-1 replication is associated with lower antiretroviral drug concentrations in lymphatic tissues. *Proc. Natl. Acad. Sci. USA* **111**, 2307–2312 (2014).

- Haase, A.T. Population biology of HIV-1 infection: viral and CD4⁺ T cell demographics and dynamics in lymphatic tissues. *Annu. Rev. Immunol.* **17**, 625–656 (1999).
- Reinhart, T.A. *et al.* Simian immunodeficiency virus burden in tissues and cellular compartments during clinical latency and AIDS. *J. Infect. Dis.* **176**, 1198–1208 (1997).
- Reinhart, T.A. *et al.* A new approach to investigating the relationship between productive infection and cytopathicity *in vivo*. *Nat. Med.* **3**, 218–221 (1997).
- Chomont, N. *et al.* HIV reservoir size and persistence are driven by T cell survival and homeostatic proliferation. *Nat. Med.* **15**, 893–900 (2009).
- Chun, T.W. *et al.* Quantification of latent tissue reservoirs and total body viral load in HIV-1 infection. *Nature* **387**, 183–188 (1997).
- Chun, T.W. *et al.* Rebound of plasma viremia following cessation of antiretroviral therapy despite profoundly low levels of HIV reservoir: implications for eradication. *AIDS* **24**, 2803–2808 (2010).
- Chun, T.W. *et al.* HIV-infected individuals receiving effective antiviral therapy for extended periods of time continually replenish their viral reservoir. *J. Clin. Invest.* **115**, 3250–3255 (2005).
- Pantaleo, G. *et al.* Lymphoid organs function as major reservoirs for human immunodeficiency virus. *Proc. Natl. Acad. Sci. USA* **88**, 9838–9842 (1991).
- Schacker, T. *et al.* Rapid accumulation of human immunodeficiency virus (HIV) in lymphatic tissue reservoirs during acute and early HIV infection: implications for timing of antiretroviral therapy. *J. Infect. Dis.* **181**, 354–357 (2000).
- Schnittman, S.M. *et al.* The reservoir for HIV-1 in human peripheral blood is a T cell that maintains expression of CD4. *Science* **245**, 305–308 (1989).
- Haase, A.T. *et al.* Quantitative image analysis of HIV-1 infection in lymphoid tissue. *Science* **274**, 985–989 (1996).
- Li, Q. *et al.* Peak SIV replication in resting memory CD4⁺ T cells depletes gut lamina propria CD4⁺ T cells. *Nature* **434**, 1148–1152 (2005).
- Schacker, T. *et al.* Productive infection of T cells in lymphoid tissues during primary and early human immunodeficiency virus infection. *J. Infect. Dis.* **183**, 555–562 (2001).
- Rothenberger, M.K. *et al.* Large number of rebounding/founder HIV variants emerge from multifocal infection in lymphatic tissues after treatment interruption. *Proc. Natl. Acad. Sci. USA* **112**, E1126–E1134 (2015).
- Lorenzo-Redondo, R. *et al.* Persistent HIV-1 replication maintains the tissue reservoir during therapy. *Nature* **530**, 51–56 (2016).
- Ho, Y.C. *et al.* Replication-competent noninduced proviruses in the latent reservoir increase barrier to HIV-1 cure. *Cell* **155**, 540–551 (2013).
- Deleage, C. *et al.* Defining HIV and SIV reservoirs in lymphoid tissues. *Pathog. Immun.* **1**, 68–106 (2016).
- Reilly, C., Wietgreffe, S., Sedgewick, G. & Haase, A. Determination of simian immunodeficiency virus production by infected activated and resting cells. *AIDS* **21**, 163–168 (2007).
- Del Prete, G.Q. *et al.* Elevated plasma viral loads in romidepsin-treated simian immunodeficiency virus-infected rhesus macaques on suppressive combination antiretroviral therapy. *Antimicrob. Agents Chemother.* **60**, 1560–1572 (2015).
- Del Prete, G.Q. *et al.* Effect of suberoylanilide hydroxamic acid (SAHA) administration on the residual viral pool in a model of combination antiretroviral therapy-mediated suppression in SIVmac239-infected indian rhesus macaques. *Antimicrob. Agents Chemother.* **58**, 6790–6806 (2014).
- North, T.W. *et al.* Viral sanctuaries during highly active antiretroviral therapy in a nonhuman primate model for AIDS. *J. Virol.* **84**, 2913–2922 (2010).
- Clements, J.E. *et al.* The central nervous system as a reservoir for simian immunodeficiency virus (SIV): steady-state levels of SIV DNA in brain from acute through asymptomatic infection. *J. Infect. Dis.* **186**, 905–913 (2002).
- Clements, J.E. *et al.* The central nervous system is a viral reservoir in simian immunodeficiency virus-infected macaques on combined antiretroviral therapy: a model for human immunodeficiency virus patients on highly active antiretroviral therapy. *J. Neurovirol.* **11**, 180–189 (2005).
- Estes, J. *et al.* Collagen deposition limits immune reconstitution in the gut. *J. Infect. Dis.* **198**, 456–464 (2008).
- Estes, J.D., Haase, A.T. & Schacker, T.W. The role of collagen deposition in depleting CD4⁺ T cells and limiting reconstitution in HIV-1 and SIV infections through damage to the secondary lymphoid organ niche. *Semin. Immunol.* **20**, 181–186 (2008).
- Schacker, T.W. *et al.* Lymphatic tissue fibrosis is associated with reduced numbers of naive CD4⁺ T cells in human immunodeficiency virus type 1 infection. *Clin. Vaccine Immunol.* **13**, 556–560 (2006).
- Schacker, T.W. *et al.* Collagen deposition in HIV-1 infected lymphatic tissues and T cell homeostasis. *J. Clin. Invest.* **110**, 1133–1139 (2002).
- Schacker, T.W. *et al.* Amount of lymphatic tissue fibrosis in HIV infection predicts magnitude of HAART-associated change in peripheral CD4 cell count. *AIDS* **19**, 2169–2171 (2005).
- Bruner, K.M. *et al.* Defective proviruses rapidly accumulate during acute HIV-1 infection. *Nat. Med.* **22**, 1043–1049 (2016).

ONLINE METHODS

Clinical and laboratory analysis (humans). HIV-infected people in Kampala, Uganda who were eligible to start ART were recruited into a longitudinal protocol conducted at the Joint Clinical Research Center (JCRC). All subjects provided written informed consent, and the institutional review boards of the University of Minnesota and JCRC and the Uganda National Council of Science and Technology (UNCST) approved the study. This was a longitudinal pathogenesis-based study with no predetermined comparators; as such, there was no predetermined sample size for recruitment.

Study procedures. At screening, peripheral blood was obtained to determine CD4 T cell counts and plasma HIV RNA levels. Just before ART initiation, all participants had an excisional inguinal lymph node biopsy, after which they were started on an ART regimen consisting of two nucleoside reverse transcriptase inhibitors (NRTI) and one non-NRTI, per the Ugandan national HIV-treatment guidelines. Subsequent CD4 T cell counts and HIV RNA levels were measured every 6 months to monitor treatment response. LN and rectal biopsies were repeated at 12, 24, and 36 months of follow-up.

Clinical and laboratory analysis (NHP). Tissues used in the described NHP studies were obtained from preexisting tissue banks or were part of additional approved studies. As such, no formal sample-size estimates were made before study design. No randomization was used to select animals for the study, and the inclusion/exclusion criteria are described below. The investigators were not blinded to the groups to which animals belonged or to the infection history or treatment regimen and duration.

Animals and SIV infection. The RMs of Indian origin (*Macaca mulatta*) used for SIV infection in these studies were mature male and female animals that ranged in age from approximately 3 to 12 years and were negative for MHC alleles associated with SIV control (Mamu A*01, B*08, and B*17). Eight RMs were housed at Advanced Bioscience Laboratories, in accordance with Association for the Assessment and Accreditation of Laboratory Animal Care (AAALAC) standards, and all procedures were performed according to protocols approved by the Advanced Bioscience Laboratories Institutional Animal Care and Use Committee (protocol no. AUP504, Office of Laboratory Animal Welfare assurance no. A3467-01). Animals at Advanced Bioscience Laboratories were intravenously (i.v.) inoculated with either 1.9×10^4 TCID₅₀ SIVmac251 (generated in the laboratory of R. Desrosiers in 2006) or 100 TCID₅₀ SIVmac251 (generated in the laboratory of R. Desrosiers in 2010). Three RMs (P568, P096, and P533) were infected with SIVmac251 (no ART) and sacrificed at 14, 43, and 90 dpi. Five additional RMs (R365, R366, R367, R406, and R410) were infected with SIVmac251 and placed on ART at 8 wpi. The ART regimen consisted of the NRTIs TFV (PMPA; 20 mg/kg; Gilead Biosciences) and FTC (50 mg/kg; Gilead Biosciences) administered subcutaneously, and the integrase strand-transfer inhibitor raltegravir (150 mg b.i.d.) plus the protease inhibitors DRV (400 mg b.i.d.) and RTV (100 mg b.i.d.), given orally. The RMs were treated for 20–22 weeks before being sacrificed. These eight RMs were used to perform a comprehensive tissue analysis of locations where SIV persisted in untreated and ART-treated infections.

The experimental conditions and ART regimens used for the 11 RMs housed at the National Cancer Institute were as previously described for five RMs (DCCN, DCHV, DCT3, DCEG, and DCJB) that received 26–32 weeks of ART beginning at 4 wpi and six RMs (DCLJ, DCT2, DCEA, DC1G, DCCP, and DCEW) that received a different regimen also begun at 4 wpi, for 31–32 weeks (refs. 22,24,25). Lymph nodes were collected by surgical extraction before (4 wpi) and 26–32 weeks after the initiation of ART (30–40 wpi) and immediately fixed in freshly prepared neutral buffered 4% paraformaldehyde for 24 h at room temperature. After fixation for 24 h, the fixative was replaced with 80% ethanol, and tissues were paraffin embedded as previously described²⁵.

Animals and RT-SHIV infection. All animals were from the retrovirus-free colony of the CNPRC, which operates according to the Guide for the Care and Use of Laboratory Animals prepared by the Committee on Care and Use of Laboratory Animals of the Institute of Laboratory Animal Resources, National Research Council. The studies were approved by the University of California,

Davis Institutional Animal Care and Use Committee. The University of California, Davis is accredited by the AAALAC. The University of California, Davis has an animal welfare assurance on file with the Office of Laboratory Animal Welfare.

Stocks of RT-SHIV were prepared as described previously²⁶. The RT-SHIV used had the T-to-C substitution at position 8 of the SIV tRNA-primer-binding site, which is necessary for efficient replication of RT-SHIV *in vivo*. Juvenile RMs 7 to 10 months of age (~2.0 to 3.1 kg) were used in the RT-SHIV study, as described by North *et al.*²⁶. Efavirenz (200 mg per day) was given in food. The NRTIs PMPA and FTC were administered subcutaneously, with a regimen of 16 mg per kg body weight once daily for FTC and 30 mg per kg body weight once daily for PMPA. The dose of PMPA was decreased to 15 mg/kg per day after 20 weeks of treatment to limit potential long-term renal toxicity associated with prolonged administration at the higher dose.

Analysis of CD4 T cell counts. For RMs, EDTA-treated whole blood was stained with monoclonal antibodies to CD3, CD4, and CD8 and analyzed with a BD FACSCalibur Flow Cytometer (BD Biosciences). Cell counts were determined with BD Trucount tubes according to the manufacturer's instructions (BD Biosciences).

For humans, blood CD4 cell counts were measured at the same time points by flow cytometry with a FACSCount system (Becton Dickinson).

Quantification of plasma viral RNA load. For RMs, plasma isolated from EDTA-treated blood of SIVmac251-infected RMs was clarified by centrifugation at 2,300g for 3 min. The clarified plasma (0.1 mL) was then lysed directly in lysis buffer (bioMerieux). Alternatively, a higher volume of plasma (0.5 to 1 mL) was centrifuged to pellet virus by ultracentrifugation at 49,100g for 60 min, and the pellet was lysed in lysis buffer. The viral RNA load in the lysed samples was quantified with a real-time NASBA assay, as previously described³⁵. Plasma SIVmac239/251 viral loads were determined as previously described, with an assay threshold of 30 copies/mL (refs. 24,25). Plasma isolated from the blood of RT-SHIV-infected challenged macaques was analyzed with previously described methods²⁶ whose lower limit of detection was 5 copies/mL.

For humans, the plasma HIV viral load was measured with the COBAS Ampliprep/COBAS TaqMan 96 (Roche) platform, with a linearity range of 20–10,000,000 copies/mL, or the Abbott m2000 platform, with a linearity range of 40–10,000,000 copies/mL. The Abbott platform was used in the first 12 months of the study, and the Roche platform was used for all subsequent measurements. Both platforms were registered in an external quality-assurance program provided by the American Pathologists and Virology Quality Assurance from Rush University Medical Center.

Procedures for initial tissue management. At the time of biopsy, each LN was dissected into two pieces. One piece was transferred to 4% paraformaldehyde for 4–6 h, then washed in 80% ethanol and embedded in paraffin and subsequently sectioned in 4-μm sections for ISH analysis.

In situ hybridization. These methods have been previously described. Briefly, for the radiolabeled and RNA/DNA scope techniques, a total of three to five 4-μm sections separated by 20 μm were analyzed by one of three ISH methods. For ISH/TSA/ELF, 10-μm sections were used.

Radiolabeled (³⁵S) in situ methods. Sections were hybridized at 45 °C overnight with a ³⁵S-labeled riboprobe and 0.5 mM aurintricarboxylic acid in the hybridization mix, with previously described methods¹⁶. After extensive washing and RNase treatment, tissue sections were dehydrated, coated in emulsion and exposed at 4 °C for 7–14 d.

ISH/TSA/ELF. These methods have been previously described^{23,36}. Briefly, sections were hybridized to digoxigenin-labeled HIV-specific antisense riboprobes with 0.5 mM aurintricarboxylic acid to decrease background. After hybridization, tissues were incubated with anti-digoxigenin antibody conjugated with HRP, extensively washed, and then incubated with biotinyl tyramine to amplify signals. The amplification step was repeated three times to detect virus particles. Tissues were then treated with streptavidin-alkaline phosphatase, and RNA signals were visualized with fluorescent ELF97 alkaline phosphatase substrate.

RNAscope/DNAscope. The antisense (for the detection of vRNA) and sense (for the detection of vDNA) SIV and HIV probes covered ~4.5 kb of the genome and were designed to bind sequences in *gag*, *pol*, *vif*, *vpx* (for SIV), *vpr*, *tat*, *rev*, *vpu* (for HIV), *env*, and *nef*, as previously described²².

Quantitative image analysis. Photographic images were captured, and the frequencies of vRNA⁺ or vDNA⁺ cells were measured and expressed as the total per unit area. These methods have been extensively reviewed^{14,18,37}.

Quantification of antiretroviral-drug concentrations. Intracellular concentrations of TFV-DP, FTC-TP, DRV, and RTV were quantified from lysed cellular matrix from PBMCs and MNCs obtained from biopsy samples of the LN, ileum (GALT), and rectum (RALT), through previously described methods^{5,38}. Final sample extracts were quantified with a liquid chromatography–triple-quadrupole mass spectrometry system consisting of a Shimadzu Nexera ultra-high-performance liquid chromatograph attached to an AB Sciex 5500 QTrap mass spectrometer. Quality-control sample interbatch coefficients of variance for the TFV-DP and FTC-TP and the DRV and RTV methods were 3.84–7.67% and 1.1–7.4%, respectively. Absolute mean relative errors to the theoretical target quality-control samples were <5.6% for TFV-DP and FTC-TP and <8.1% for DRV and RTV. The batch acceptance criterion was derived according to the Food and Drug Administration Guidance for Industry on Bioanalytical Method Validation³⁹. The results from intracellular analyses are expressed in femtomoles per million cells. The relative penetration of the ARVs into the LN, GALT, and RALT was assessed as a ratio of concentrations to those in PBMCs.

Statistical analysis. Data presented from individual animals to describe the frequency of vRNA or vDNA⁺ cells are expressed as the total number of cells per g tissue for that organ in that animal (for example, **Figs. 2 and 3**). Analyses of differences between tissue sites, or before and during ART, were made by comparing the means of the two groups with ANOVA (for example, **Fig. 6**).

Data availability. All data are available from the authors upon reasonable request. A **Life Sciences Reporting Summary** for this paper is available.

35. Lee, E.M. *et al.* Molecular methods for evaluation of virological status of nonhuman primates challenged with simian immunodeficiency or simian-human immunodeficiency viruses. *J. Virol. Methods* **163**, 287–294 (2010).
36. Zhang, Z.Q. *et al.* Roles of substrate availability and infection of resting and activated CD4⁺ T cells in transmission and acute simian immunodeficiency virus infection. *Proc. Natl. Acad. Sci. USA* **101**, 5640–5645 (2004).
37. Cavert, W. *et al.* Kinetics of response in lymphoid tissues to antiretroviral therapy of HIV-1 infection. *Science* **276**, 960–964 (1997).
38. Podany, A.T., Winchester, L.C., Robbins, B.L. & Fletcher, C.V. Quantification of cell-associated atazanavir, darunavir, lopinavir, ritonavir, and efavirenz concentrations in human mononuclear cell extracts. *Antimicrob. Agents Chemother.* **58**, 2866–2870 (2014).
39. Guidance for Industry. *Bioanalytical Method Validation* (U.S. Department of Health and Human Services, 2001).

Life Sciences Reporting Summary

Nature Research wishes to improve the reproducibility of the work we publish. This form is published with all life science papers and is intended to promote consistency and transparency in reporting. All life sciences submissions use this form; while some list items might not apply to an individual manuscript, all fields must be completed for clarity.

For further information on the points included in this form, see [Reporting Life Sciences Research](#). For further information on Nature Research policies, including our [data availability policy](#), see [Authors & Referees](#) and the [Editorial Policy Checklist](#).

► Experimental design

1. Sample size

Describe how sample size was determined.

Non-Human Primate: These are observational studies based largely on archival tissue samples from other experiments.
Human: These tissues are from an observational study of volunteers initiating ART in Kampala, Uganda. No formal sample-size calculations were made.

2. Data exclusions

Describe any data exclusions.

None

3. Replication

Describe whether the experimental findings were reliably reproduced.

Yes, we have a rigorous process for verifying QIA results including 2 different individuals completing analysis on randomly selected images to maintain quality control.

4. Randomization

Describe how samples/organisms/participants were allocated into experimental groups.

not applicable

5. Blinding

Describe whether the investigators were blinded to group allocation during data collection and/or analysis.

None

Note: all studies involving animals and/or human research participants must disclose whether blinding and randomization were used.

6. Statistical parameters

For all figures and tables that use statistical methods, confirm that the following items are present in relevant figure legends (or the Methods section if additional space is needed).

- | | |
|-------------------------------------|--|
| n/a | Confirmed |
| <input checked="" type="checkbox"/> | <input type="checkbox"/> The <u>exact</u> sample size (n) for each experimental group/condition, given as a discrete number and unit of measurement (animals, litters, cultures, etc.) |
| <input type="checkbox"/> | <input checked="" type="checkbox"/> A description of how samples were collected, noting whether measurements were taken from distinct samples or whether the same sample was measured repeatedly. |
| <input checked="" type="checkbox"/> | <input type="checkbox"/> A statement indicating how many times each experiment was replicated |
| <input type="checkbox"/> | <input checked="" type="checkbox"/> The statistical test(s) used and whether they are one- or two-sided (note: only common tests should be described solely by name; more complex techniques should be described in the Methods section) |
| <input type="checkbox"/> | <input checked="" type="checkbox"/> A description of any assumptions or corrections, such as an adjustment for multiple comparisons |
| <input type="checkbox"/> | <input checked="" type="checkbox"/> The test results (e.g. p values) given as exact values whenever possible and with confidence intervals noted |
| <input type="checkbox"/> | <input checked="" type="checkbox"/> A summary of the descriptive statistics, including central tendency (e.g. median, mean) and variation (e.g. standard deviation, interquartile range) |
| <input type="checkbox"/> | <input checked="" type="checkbox"/> Clearly defined error bars |

See the web collection on [statistics for biologists](#) for further resources and guidance.

► Software

Policy information about [availability of computer code](#)

7. Software

Describe the software used to analyze the data in this study.

Photoshop, Prism, Microsoft Excel

For all studies, we encourage code deposition in a community repository (e.g. GitHub). Authors must make computer code available to editors and reviewers upon request. The *Nature Methods* [guidance for providing algorithms and software for publication](#) may be useful for any submission.

► Materials and reagents

Policy information about [availability of materials](#)

8. Materials availability

Indicate whether there are restrictions on availability of unique materials or if these materials are only available for distribution by a for-profit company.

No restriction

9. Antibodies

Describe the antibodies used and how they were validated for use in the system under study (i.e. assay and species).

not applicable

10. Eukaryotic cell lines

a. State the source of each eukaryotic cell line used.

not applicable

b. Describe the method of cell line authentication used.

not applicable

c. Report whether the cell lines were tested for mycoplasma contamination.

not applicable

d. If any of the cell lines used in the paper are listed in the database of commonly misidentified cell lines maintained by [ICLAC](#), provide a scientific rationale for their use.

Provide a rationale for the use of commonly misidentified cell lines OR state that no commonly misidentified cell lines were used.

► Animals and human research participants

Policy information about [studies involving animals](#); when reporting animal research, follow the [ARRIVE guidelines](#)

11. Description of research animals

Provide details on animals and/or animal-derived materials used in the study.

Rhesus macaques of Indian origin (*Macaca mulatta*; RMs) used for SIV infection in these studies were mature male and female animals ranging in age from approximately 3–12 years, and were negative for MHC alleles associated with SIV control (Mamu A*01, B*08, and B*17). Eight RMs were housed at Advanced Bioscience Laboratories (ABL) in accordance with the Association for the Assessment and Accreditation of Laboratory Animal Care (AAALAC) standards and all procedures were performed according to protocols approved by the ABL Institutional Animal Care and Use Committee (IACUC) (Protocol # AUP504, OLAW Assurance #A3467-01). Animals at ABL were intravenously (i.v.) inoculated with either 1.9×10^4 TCID₅₀ SIVmac251 (generated in the laboratory of Dr. Ron Desrosiers during 2006) or 100 TCID₅₀ SIVmac251 (generated in 2010 in the laboratory of Dr. Ron Desrosiers). Three RMs (P568, P096, and P533) were infected with SIVmac251 (no ART) and sacrificed at 14, 43, and 90 days post infection. Five additional RMs (R365, R366, R367, R406 and R410) were infected with SIVmac251 and placed on ART at 8 wpi started on an ART regimen that consisted of the NRTIs tenofovir (PMPA; 20 mg/kg; Gilead Biosciences) and emtricitabine (FTC; 50 mg/kg; Gilead Biosciences) administered subcutaneously, and the integrase strand transfer inhibitor raltegravir (RAL; 150mg BID) plus the protease inhibitors darunavir (DRV; 400 mg; BID) and ritonavir (RTV; 100 mg; BID) given orally; and treated for 20–22 weeks prior to being sacrificed. These 8 RMs were utilized to perform a comprehensive tissue analysis of where SIV persisted in untreated and ART treated infection.

The experimental conditions and ART regimens employed for the 11 rhesus macaques housed at the National Cancer Institute were previously described for 5 RM (DCCN, DCHV, DCT3, DCEG, and DCJB) which received 26–32 weeks of ART beginning at 4 weeks post-infection and 6 RM (DCLJ, DCT2, DCEA, DC1G, DCCP and DCEW) which received a different regimen and also begun at 4 weeks post-infection, for 31–32 weeks. 22, 24, 25 Lymph nodes were collected by surgical extraction before (4 wpi) and 26–32 weeks after the initiation of ART (30–40 wpi) and immediately fixed in freshly prepared neutral buffered 4% paraformaldehyde (PFA) for 24 h at room temperature. After fixation for 24 h, fixative was replaced with 80% ethanol and tissues were paraffin embedded as previously described.

Policy information about [studies involving human research participants](#)

12. Description of human research participants

Describe the covariate-relevant population characteristics of the human research participants.

HIV-infected people in Kampala, Uganda who were eligible to start ART were recruited into a longitudinal protocol that was conducted at the Joint Clinical Research Center (JCRC). All subjects gave written informed consent and the Institutional Review Boards (IRB) of the University of Minnesota and JCRC and the Uganda National Council of Science and Technology (UNCST) approved the study. This was a longitudinal pathogenesis based study with no pre-determined comparators, as such we did not have a pre-determined sample size for recruitment.